Critical role of boundary conditions in sorption kinetics measurements

Yuliang Zou, Luoyi Yan, Benjamin Maillet, Rahima Sidi-Boulenouar, Laurent Brochard, Philippe Coussot

The critical role of boundary conditions in sorption kinetics measurements

Yuliang Zou, Luoyi Yan, Benjamin Maillet, Rahima Sidi-Boulenouar, Laurent Brochard, and Philippe Coussot*

Laboratoire Navier (Ecole des Ponts Paris Tech-Univ Gustave Eiffel-CNRS), Champs-sur-Marne, France

E-mail: philippe.coussot@univ-eiffel.fr

Abstract

In order to characterize the hygroscopic properties of cellulose-based materials, which can absorb large amounts of water from vapor in ambient air, or the adsorption capacity of pollutants or molecules in various porous materials, it is common to rely on sorption-desorption dynamic tests. This consists in observing the mass variation over time when the sample is placed in contact with a fluid containing the elements to be absorbed or adsorbed. Here, we focus on the case of a hygroscopic material in contact with air at a relative humidity (RH) differing from that at which it has been prepared. We show that the vapor mass flux going out of the sample follows from the solution of a vapor convection-diffusion problem along the surface, and is proportional to the difference between the RH of the air flux and that along the surface with a multiplicative factor (δ) depending only on the characteristics of the air flux and the geometry of the system, including the surface roughness. This factor may be determined from independent measurements in which the RH along the surface is known, while keeping all other variables constant. Then we show that the apparent

sorption or desorption kinetics critically depends on the competition between boundary conditions and transport through the material. For sufficiently low air flux intensities or small sample thicknesses, the moisture distribution in the sample remains uniform and evolves towards the equilibrium with a kinetics depending on the value of δ and of the material thickness. For sufficiently high air flux intensities or large sample thicknesses, the moisture distribution is highly inhomogeneous and the kinetics reflects the ability of water transport by diffusion through the material. We illustrate and validate this theoretical description on the basis of MRI (Magnetic Resonance Imaging) experiments on drying cellulose fiber stacks.

Nomenclature

α	Coefficient of pore coverage (with water)
$\bar{J}$	Average vapor flux over the surface
δ	Characteristic thickness of the boundary layer for vapor diffusion
μ	Air viscosity
Re	Reynolds number
ρ	Air density
Sc	Schmidt number
ε	Material porosity
ξ	Dimensionless surface roughness
ζ	Surface roughness
A	Area of the sample cross-section

B Dimensionless number comparing vapor diffusion through the boundary layer to bound water diffusion through the sample

D Diffusion coefficient of bound water through the sample

f Undetermined function of the variables or parameters in brackets

H Sample thickness

h Mass transfer coefficient

J Vapor mass flux from the sample surface

L Characteristic length of the sample surface

n Relative humidity (RH)

R Characteristic pore size

S Moisture content

s Concentration of bound water

t Time

t^* Dimensionless time

u Velocity component along the direction x (tangential velocity)

V Characteristic velocity of the air flux

x Direction along sample-air interface

y Direction of the sample axis, perpendicular to sample surface

ρ_0 Saturation vapor density

ρ_s Density of the dry sample

D_0 Diffusion coefficient of vapor through the air

M_∞ Total water mass transfer at equilibrium

M_t Total mass transfer at time t

n^* Reduced relative humidty

n_0 Relative humidity during sample preparation

n_∞ Relative humidity in the incident air flux

n_s Relative humidity at the sample-air interface

S_0 Initial sample moisture content

s_0 Initial bound water concentration in sample

S_m Maximum moisture content in sample

T^* Characteristic time of diffusion

u^* Dimensionless tangential velocity

x^*, y^* Dimensionless distance variables

Introduction

Wood, plants, natural textiles, paper, and bio-based construction materials are cellulosic materials, a specificity of which is to be hygroscopic. This property means that they are capable of absorbing water vapor from the ambient air, a reversible process. This absorbed water is the so-called "bound water",[1–4] which can amount to 30% of the dry mass. In contrast with molecules or particles adsorbing onto the surface of various materials[5] this bound water essentially forms by entering the amorphous regions between cellulose microfibrils[3,4] thanks to the high sorption affinity of the cellulose chains for water molecules in particular

near their polar OH groups.[1–3] This bound water is thus confined in nanopores that it has itself created, which is at the origin of the swelling or shrinkage of such materials.

This property, in particular, plays a major role in the hygrothermal properties of these materials. In this context, natural textiles (cotton, flax, hemp, jute, wool, etc.) for clothes,[6,7] and bio-based construction materials such as wood or insulation materials (fiber stacks of wheat, flax, wood, bamboo, coir, etc.),[8–11] are particularly interesting as they can absorb, store, or restitute humidity, thus ensuring moisture buffering in the surroundings. Standard characterizations of the hygroscopic properties of these materials rely on sorption or desorption tests, which consist in observing the bound water mass variation when the sample is placed in ambient air at a RH (Relative Humidity, noted n) differing from that at which it has been prepared. This, in particular, provides the sorption (or desorption) curve corresponding to the moisture content, i.e., the bound water to dry mass ratio (noted S), as a function of RH, at equilibrium. The knowledge of the kinetics of the sorption process, i.e., the time variation of the absorbed mass under specific conditions, is also essential as it provides the characteristic time for a material to become wet (with bound water) under a high RH, to dry under a low RH, or the characteristic time needed for a textile or construction material to absorb the humidity of a room.

There is a similar issue for the characterization of the sorption kinetics of molecules onto the solid surface of various porous materials such as silica particles or composites sorbents,[12,13] TiO2 films,[14] aluminophosphate layers,[15] metal organic framework,[13,16] resins,[17] polymer composites,[18,19] zeolites,[20] Carbon,[21] or of water penetration in clay[22] or cereals.[23]

Typically, in order to measure the sorption kinetics, a sample of material is placed in a climatic chamber supposed to be able to maintain the air around the sample at a given value of RH, i.e., n_∞, while the material has been prepared under a different RH, i.e., n_0.[12,19,21,24–26] The sorption dynamics of the material is then expected to depend on n_∞ and n_0, and is described through the relative variation of the sample mass in time. In that case, it is implicitly assumed that there is negligible air flow and, for the relevance of the theoretical

analysis, that the boundary condition, i.e., the relative humidity along the surface of the sample remains equal to the ambient one, i.e., n_∞. However, this humidity is only controlled via a sensor at a significant distance from the sample surface, generally along a wall of the chamber (see Figure 1).

Alternatively, a dynamic vapor sorption (DVS) apparatus is often used,[23,27–29] in which a Nitrogen-vapor mixture is flowed around the sample placed in a chamber, while the RH is controlled in the surroundings of the sample, but not along the sample surface. Again here, the sample mass variations over time under such conditions are considered to reflect the sorption kinetics of the material. In the same vein, it was suggested[30] that one can appreciate the MBV (Moisture Buffer Value, i.e., the ability of a material to moderate the variations of indoor humidity in buildings) by performing a test that consists in imposing alternatively low and high humidities over several days.[31–38]

When the DVS, the MBV tests, or other tests of the hygrothermal properties of materials, have been interpreted theoretically, it appeared necessary to express the boundary condition in a more subtle way than for tests in climatic chambers, now taking into account the air flow along the interface. It is then generally considered that this boundary condition may be formulated by expressing the water mass flux through the interface, i.e., J, in the form $J = h(n_\infty - n_s)$ in which n_s is the RH along the interface.[39–43] Note that here h is an unknown coefficient that depends on the flow characteristics and the sample geometry, but it is also often assumed to depend on other material properties, which is illustrated by the fact that it was called the "surface resistance" or "surface emission" coefficient.[23,44–46] In addition, n_s is generally considered as constant during the process, which is somewhat in contradiction with the fact that the water content absorbed in the material evolves over time. More complex boundary conditions were also proposed, such as first-order kinetic equations.[47,48] Within the frame of a farsighted work, Thorell[40] finally suggested that the value of this coefficient might be determined from independent tests using a water-saturated sample. There is thus a need to clarify the physical origin of this boundary condition, which is our first objective

in this paper.

Whatever the boundary conditions, the physical interpretation of the sorption kinetics for hygroscopic materials remains problematic. In their review of physical phenomena that occur during the sorption process, Thybring et al.[49] remarked that both external resistance to vapor transfer and bound water diffusion in cell walls might play a role, but they finally concluded that no previously developed model can phenomenologically describe the sorption process. In particular, it was remarked[49–51] that some characteristics of the PEK (Parallel Exponential Kinetics) model, an empirical two-exponential model fitted to data,[28,52–55] can depend on experimental conditions. Also, various contradictions with the predictions of a simple diffusion process were observed.[49,51,56] However, let us recall that boundary conditions, which are not necessarily well taken into account, have a critical impact on the characteristics of a diffusion process.[57] Pichler's work,[39] focused on sandstone, provided critical observations and analysis for understanding the origin of such discrepancies. Indeed, they demonstrated that with thin samples the mass transfer is determined almost entirely by the surface resistance (with quasi-instantaneous transport within the body), whereas in thick samples surface effects become negligible. These observations clearly show the challenge of interpreting the sorption kinetics observed in such tests as reflecting some intrinsic properties of the material.

Actually, this point has already been well identified within the framework of sorption of pollutants in porous materials, leading to the conclusion that a sorption process relies on several steps: transport of adsorbate in the bulk solution around the particles, diffusion of adsorbate inside the pores, and surface adsorption or desorption.[17,58] This leads to interpreting sorption kinetics data taking into account the diffusion process inside the material along with the exchange with the solid surface.[13,16–18,21,58] However, in those cases, simplified boundary conditions (such as constant adsorbate concentration along the free surface of the material) are generally assumed, despite the complex shape of the sample (typically in the form of pellets or powder) and the poor control of the fluid flux along the sample.

Here, we emphasize the need to carry out controlled experiments for measuring the sorption kinetics of materials, and in particular to properly take into account boundary conditions to ascertain the theoretical interpretations. We will focus on the case of water sorption or desorption in hygroscopic materials, and more precisely a model cellulosic system, keeping in mind that the general concepts developed within this framework would be applicable to any type of sorption process.

Let us consider a desorption mechanism, associated with $n_\infty < n_0$, while a sorption mechanism is simply the inverse situation. First of all, we note that the desorption process results from the gradient of relative humidity existing between the sample surface and the surrounding air. This desorption will start from the air-sample interface and propagate inside the sample. This propagation results from the transport of water from the deep layers to the surface, a transport that is due to a gradient of moisture content. Thus, regardless its physical origin (it may involve several physical effects such as bound water and vapor diffusion), since it occurs spontaneously as a result of a concentration gradient, this water transport is a diffusion process.[57,59]

This diffusion process is more or less complex essentially depending on the variations of the diffusion coefficient with the moisture content. This may be studied through experiments providing an insight into the moisture content distribution in the sample. Some information may also be obtained from simpler macroscopic experiments such as those above described. However, to interpret the results of these tests, as for any diffusion problem, it is critical to control the boundary conditions. This control means: 1) to impose constant boundary conditions, and 2) to know their impact on the conditions along the sample-air interface.

As a consequence, here we start by reviewing in detail the boundary conditions resulting from an air flux along a sample-air interface. In particular, we show that a general expression may be derived, the parameters of which may be determined with the help of an independent experiment. We also show that these parameters are not dependent on the material characteristics. As a next step, we proceed to solve the complete set of equations

including the diffusion equation and the boundary condition. We show that the effective value of the relative humidity along the interface in fact depends on the coupling between the air flux and the diffusion in the material. Two asymptotic regimes then appear, which will be obtained depending on the air flux intensity and the sample thickness. Depending on the regime in which the desorption kinetics experiment is carried out, the result can be either mostly controlled by or almost independent of the diffusion properties in the material. We illustrate these results by a comparison with experimental data with a cellulose fiber stack. Finally, we propose practical considerations for carrying out relevant measurements of sorption kinetics.

Imposing a given RH in a room – Resulting boundary condition

Let us consider an equipment, such as a climatic chamber or a DVS apparatus, which imposes some given temperature and relative humidity values in the surroundings (which we call chamber) of a material sample. The gas around the sample may for example be air or nitrogen, and for the sake of simplicity, we call in any case relative humidity the ratio of vapor concentration to the saturation concentration which is the maximum possible vapor concentration in this gas at this temperature. First of all, since the control of these variables is carried out thanks to some sensors located in specific points inside the chamber the temperature and RH values may be different in other places, in particular very close to the sample surface. Secondly, since there are some heat exchanges with the external air through the walls of the equipment and humidity exchanges between the gas inside the chamber and the sample, the system needs to continuously readjust the temperature and humidity of the gas inside the chamber. A simple diffusion process being in general slow, the technique generally used is the injection of a gas flux in the interior volume (see Figure 1).

The need for gas renewal in the chamber implies that the gas in the chamber moves.

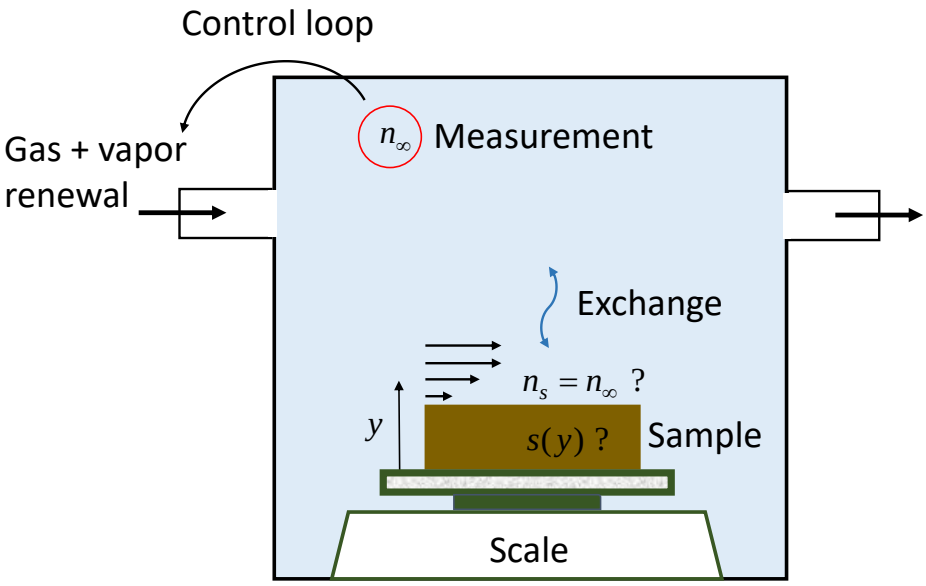

Figure 1: Scheme of the principle of a sorption test in a climatic chamber or in a DVS apparatus: one imposes, with a control loop, the ambient RH to n_∞, with adjusted gas and vapor renewal, while there is some exchange of humidity between the ambient gas and the sample. Due to the resulting gas flow along the sample, one may wonder whether the effective value of RH along the sample surface is n_∞, and due to the water diffusion in the sample one may wonder whether the variation of RH along the sample depth plays a role, in particular in the resulting value of n_s. These considerations apply to the spatial distribution of temperature in a similar way.

The resulting flow characteristics are a priori complex, as they depend on the details of the geometry of the interior of the chamber, on the point of injection, on the rate at which it is injected, etc. Thus, we ignore the details of this motion, but at least we know that if the sample has essentially one planar surface in contact with the gas, close to this surface the gas will necessarily move tangentially to it, as it can hardly penetrate the sample which is lying over a non-permeable surface. This implies that a boundary layer for the RH distribution forms along the surface, analogous to the boundary layer for the velocity: a gas flux with a homogeneous RH distribution reaching the edge of the surface will then move along this surface while exchanging water with the sample through the interface (see Figure 2); the vapor distribution is then progressively modified as the gas advances along the surface; at the edge ($x = 0$) the RH at the surface ($y = 0$) is now n_s, while it is still equal to n_∞ for $y > 0$, which induces a strong gradient of RH; this gradient then progressively softens

for increasing distance from $x = 0$, as the vapor moves away from the surface, so that the thickness of the region in which n differs from n_∞ increases with x (see Figure 2).

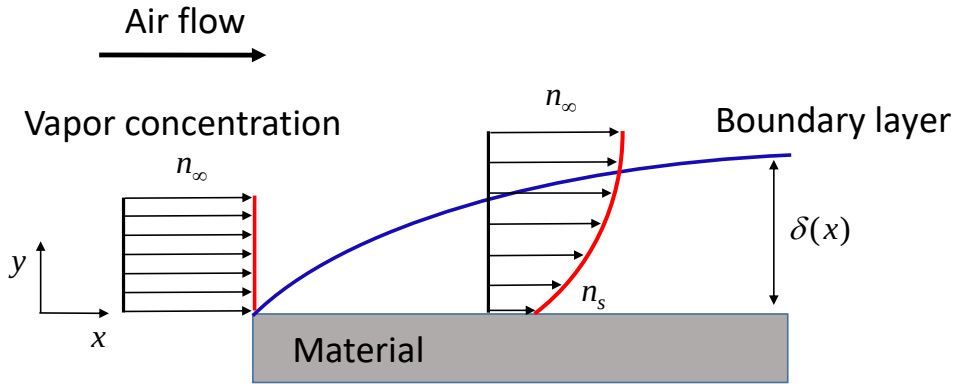

Figure 2: Boundary layer of vapor concentration resulting from air flow along a material surface. δ is the characteristic distance of diffusion of vapor through air from the interface, i.e., roughly the distance over which one observes the main variations of the RH from the surface of the material

Thus, we are basically faced with the problem of vapor diffusion through an air (or another gas) flow moving tangentially to the free surface of the sample. Here we will analyze the problem in a general way, i.e., for any type of flow along the surface, not specifically for conditions corresponding to the simple tangential flow shown in Figure 2. We focus on the flow along the surface, since this the meaningful characteristics in terms of resulting evaporation rate. Thus, we consider any type of flow along the surface resulting from any effective boundary conditions associated with some air flux arriving around the sample. We consider isothermal conditions, which amounts to considering that the processes evolve sufficiently slowly for the system to be always at equilibrium with the ambient temperature (the air flux being at the same temperature as the initial sample temperature). Moreover, we can assume a steady-state flow, as the possible variations of the air flow (induced by the equipment), say over a few minutes, are much slower than the characteristic time of the flow itself, i.e., the order of seconds or smaller (a few centimeters per second to cover a length in the order of centimeters). For the sake of simplicity, we describe the flow characteristics in a plane (x, y), in which x is the direction of the tangential flow, and y is the axis perpendicular

to the surface. We assume that gravity effects are negligible, and that the sample edge is far from the point of air flux arrival (or departure) along the surface, so that there is only one non-zero velocity component, u, along the direction x. Under these conditions, the flow characteristics are fully described by the mass and momentum conservation equations along with the boundary conditions, and a similarity analysis shows[60] that the dimensionless tangential velocity $u^* = u/V$ may be expressed in the form:

$$u^* = f(x^*, y^*, \mathrm{Re}, \xi). \tag{1}$$

Here we use the generic symbol f to represent an undetermined function of the variables or parameters in brackets. V is a characteristic velocity of the air flux, which may for example be the mean velocity of the air flux at its arrival on the surface (i.e., for $x = 0$), $x^* = x/L$; $y^* = y/L$ are dimensionless distance variables, in which L is a characteristic length of the sample surface (typically the surface extent in the direction x), and $\mathrm{Re} = \rho V L/\mu$ is the Reynolds number, in which ρ and μ are the air density and viscosity, and $\xi = \zeta/L$ is the dimensionless surface roughness (with ζ the roughness). Note that formally the expression 1 is valid for a laminar and a turbulent flow, but the roughness may play a role essentially in the case of a turbulent flow.

Let us now consider more precisely that the air arrives onto this surface at a RH of n_∞ and flows along this planar surface of material along which the RH is maintained at n_s. Since there is a gradient of humidity in the air above the surface we expect a diffusion of vapor, but at the same time, this vapor is convected along the x direction. The vapor transport in the air region ($y > 0$) is described by the mass conservation equation for vapor leading to a convection-diffusion equation which, in the absence of vapor source in this region, writes:

$$\frac{\partial n}{\partial t} + u\frac{\partial n}{\partial x} = D_0 \frac{\partial^2 n}{\partial y^2}, \tag{2}$$

in which D_0 is the diffusion coefficient of vapor through the air. Note that in this equation

the second term of diffusion $D_0\partial^2 n/\partial x^2$ has been removed as it is in general far negligible compared to the term $u\partial n/\partial x$, due to a very large Peclet number VL/D_0.

A similarity analysis of this equation[60,61] in steady-state leads to the following expression for the rescaled relative humidity

$$n^* = f(x^*, y^*, u^*, \mathrm{ReSc}), \tag{3}$$

in which $n^* = \frac{n-n_s}{n_s-n_\infty}$ and $\mathrm{Sc} = \frac{\mu}{\rho D_0}$ is the Schmidt number.

Taking into account in equation 3 the expression 1 for u^* we finally obtain an expression of the form

$$n^* = f(x^*, y^*, \mathrm{Re}, Sc, \xi). \tag{4}$$

Let us now consider the vapor mass flux in the direction y resulting from the concentration gradient. Since at $y = 0$ the vapor has not already been transported along the sample surface, this flux along the sample surface (i.e., $y = 0$) represents the total vapor mass extracted from (or stored by) the sample per unit surface and time. From the first Fick's law, it writes

$$J(x) = -\rho_0 D_0 \left(\frac{\partial n}{\partial y}\right)_{y=0} = -\rho_0 \frac{D_0}{L}\left(n_s - n_\infty\right)\left(\frac{\partial n^*}{\partial y^*}\right)_{y^*=0}, \tag{5}$$

in which ρ_0 is the saturation vapor density at the temperature under consideration. From (4) we deduce $\left(\partial n^*/\partial y^*\right)_{y^*=0} = f(x^*, \mathrm{Re}, Sc, \xi)$, and the average vapor flux over the surface, i.e., for x between 0 and L, writes

$$\bar{J} = \frac{1}{L}\int_0^L J dx = \left[f(\mathrm{Re}, Sc, \xi)\right]\rho_0 \frac{D_0}{L}\left(n_s - n_\infty\right). \tag{6}$$

In the following, we simply use the symbol J to express the average vapor flux. Note that an expression formally similar to 6 would be obtained by considering the full velocity field in three dimensions, by using a function f now depending additionally on the direction z^* and integrating over the whole sample surface (including all possible values of x^* and z^*).

Also note that the above calculation assumes that at each instant the value n_s is uniform along the sample surface, which is obviously not strictly exact since the local flux varies with x according to equation 5. However, we here assume that the air flux characteristics and the sample properties are such that these variations are limited and/or partially balanced by some internal transports, so that at first order the assumption of moisture content independent of x in the sample, and in particular at its surface, is valid. This seems consistent with data obtained by MRI for a drying cellulose paste: in the last stage of drying, when there is only bound water in the sample, the 2D longitudinal images of the sample show no significant heterogeneity along sample cross-sections.[62] This assumption is important as it will allow us to consider the diffusion process described in the next section as a unidirectional process.

The average flux may also be written

$$J = h\,(n_s - n_\infty)\,, \tag{7}$$

with

$$h = f(\frac{\rho V L}{\mu}, \frac{\mu}{\rho D_0}, \xi)\rho_0 \frac{D_0}{L}. \tag{8}$$

The expression (7) for the vapor flux contains the linear dependence on $(n_s - n_\infty)$ typically assumed in various approaches (see Introduction), but with the factor h being an unknown parameter, nevertheless often considered as depending on some material property and named either convective mass transfer coefficient or coefficient of exchange or emission. In fact, the above straightforward theoretical approach clearly shows that this coefficient only depends on the characteristics of the air flux, namely its density, velocity, viscosity, the diffusion coefficient of vapor through air, and the geometry of the system (through L, ξ, and the function f). Note that these parameters negligibly vary with the RH. Thus, this coefficient h definitely does not depend on any intrinsic material property. The material characteristics only play a role through the roughness of the free surface of the sample, but, to some extent, this roughness may be adjusted. As we will see below, some intrinsic material

characteristics, and more particularly the diffusion properties, play a role in the observed vapor transport only because they impact the value of n_s, but not through the factor h which only depends on the air flow characteristics and its boundary conditions.

One can also rewrite the vapor flux in the following more physical form:

$$J = \rho_0 \frac{D_0}{\delta} \left(n_s - n_\infty \right), \tag{9}$$

in which δ would be an equivalent thickness of air through which the vapor would freely (without convection) diffuse from the material surface to a region at humidity n_∞, with

$$\delta = \frac{L}{f(\frac{\rho V L}{\mu}, \frac{\mu}{\rho D_0}, \xi)}. \tag{10}$$

Obviously, the same conclusions as for h apply to δ: it only depends on the air flux characteristics and geometry of the system. Thus, as drying affects the water content in the porous material, n_s may evolve in time, which can modify the boundary conditions, i.e., the vapor mass flux extracted through the air-material interface (through (9), but fundamentally the characteristic distance δ of diffusion does not change during this process if the supplied air flux remains constant.

As an important practical corollary, although the function f may be a complex function of the system parameters and in particular its exact geometrical characteristics, in practice, δ may be estimated by measuring the vapor flux under controlled conditions, i.e., when n_s is known, for example in the initial state. For example, let us consider a hygroscopic sample prepared at some RH n_0, i.e., left for sufficient time until reaching equilibrium. By definition, the initial moisture content at any point in the sample is S_0, corresponding to the equilibrium state $S_0(n_0)$ in the sorption (or desorption) curve, and in this state the RH in the air surrounding any point of the material is n_0. This is in particular the case of the initial relative humidity just along the sample surface, in contact with the first material layers, which will be equal to n_0. If now the sample is placed in contact with an air flux at

a different RH n_∞, the (initial) vapor flux will be J_0, defined by 9, from which we deduce $\delta = \rho_0 \left(D_0/J_0\right)(n_0 - n_\infty)$. Finally, this value may be used to express the vapor flux at any time, i.e., when the RH along the surface is now n_s:

$$J = J_0 \frac{n_s - n_\infty}{n_0 - n_\infty}. \tag{11}$$

We can get a rough idea of the variation of δ with V by considering the simplistic case of a uniform air flow at a velocity V along the sample surface. This means that we neglect the development of the boundary layer of the air flux itself. In that case, the steady-state vapor distribution is described by the convection-diffusion equation $V\partial n/\partial x = D_0 \partial^2 n/\partial y^2$, which is equivalent to a simple diffusion equation after a change of variable to $t = x/V$, whose solution is

$$n(x, y) = n_s + (n_\infty - n_s)\,\mathrm{erf}\left(\frac{y}{2\sqrt{D_0 x/V}}\right). \tag{12}$$

As a consequence, for a given position y the local vapor flux in the direction normal to the surface writes $J = -\rho_0 D_0 \left(\frac{\partial n}{\partial y}\right)_{y=0} = \frac{\rho_0 D_0}{\sqrt{\pi D x/V}}(n_s - n_\infty) = \rho_0 D_0 \frac{n_s - n_\infty}{d}$, with $d = \sqrt{\pi D_0 x/V}$, and over a length L the total vapor flux writes $J = \rho_0 D_0 \frac{n_s - n_\infty}{\delta}$, with

$$\delta = \left(\frac{1}{L}\int_0^L \frac{dx}{\sqrt{\pi D_0 x/V}}\right)^{-1} = \frac{1}{2}\sqrt{\frac{\pi D_0 L}{V}}. \tag{13}$$

As expected, δ is found to increase with the length of the surface, and to decrease with the velocity of the air flux, but we see that these variations are rather slow, typically scaling with the square root of these variables. In particular, this means that the heterogeneity of δ along the sample surface is somewhat limited.

Summary of findings

- The vapor mass flux going out of the sample is proportional to the difference between the RH of the air flux and along the surface with a factor $(\rho_0 D_0/\delta)$ which only depends

on the characteristics of the air flux, namely its density, velocity, viscosity, the diffusion coefficient of vapor through air, and the geometry of the system, including the surface roughness.

- This vapor mass flux may thus change during the process only if the RH along the surface changes, as a result of the extraction of water from the material.

- The factor $\rho_0 D_0/\delta$ may be estimated from independent tests in which the RH along the surface is known, all other things being equal.

Coupling with the diffusion process in the material

The above analysis shows that it is possible to predict (cf. equation (11)) the rate of extraction of water by evaporation from the surface of a material subjected to a tangential air flux as soon as one knows the initial drying rate and the current value of the relative humidity along this surface. Actually, this relative humidity n_s is related to the moisture content in the sample along this surface, i.e., S_s. Here, for the sake of simplicity, we will consider a unique function, i.e., $S = S(n)$ for the sorption and desorption curves. Indeed, no significant difference can be observed in the data for sorption or desorption measurements with different cellulosic materials at equilibrium,[63,64] and a unique function is found to relate moisture content and RH. One could extend what follows to the case of sorption hysteresis, by distinguishing the adsorption and desorption isotherms. Then, exactly along the interface $y = 0$, we have a sorption equilibrium due to the very fast exchange of water molecules over an infinitely small material thickness. Thus we have $S_s = S(y = 0^-) = S(n_s)$. In the general case, we impose an air flux at a RH n_∞ differing from the RH associated with sorption equilibrium in the sample, i.e., $n_0 = S^{-1}(S_0)$, in which S_0 is the initial moisture content of the sample. This implies that the initial value of n_s (i.e., $n_s = S^{-1}(S_0)$) will differ from n_∞, leading to a non-zero vapor mass flux through the interface. This induces a variation of S_s, which then differs from S_0.

This difference in moisture content between two different regions of the sample induces a diffusional transport. We naturally assume that this may be described by a standard diffusion process with a diffusion coefficient D, possibly depending on the moisture content. Neglecting the sample deformations induced by water absorption, the density of bound water in the sample is $\rho_s S$, where ρ_s is the density of the dry sample (and not the density of the solid fibers). We then define $s = S/S_m$, which corresponds to a concentration of bound water, i.e., the ratio of the bound water mass to its maximum value S_m, and with reference to the usual term in porous media, we call it saturation. We assume the sample cross-section is sufficiently large compared to its thickness and/or edge effects are negligible (negligible transport through sidewalls) so that the variables only depend on the position y. The evolution of s in the sample is then described by a diffusion equation:

$$For \quad y < 0, \quad \frac{\partial s}{\partial t} = \frac{\partial}{\partial y}\left(D(s)\frac{\partial s}{\partial y}\right), \tag{14}$$

with a boundary condition resulting from the equality of the internal ($y = 0^-$) and external ($y = 0^+$) fluxes along the interface $y = 0$:

$$-\rho_s S_m D\frac{\partial s}{\partial y} = -\frac{\rho_0 D_0}{\delta}(n_\infty - n_s). \tag{15}$$

The equation (14) with the boundary condition (15) and in general the assumption of no mass flux through the sample bottom, along with the initial condition $s = s_0$ and the knowledge of the sorption curve $S(n) = sS_m$, may be solved numerically. However, the equation (15) may be rewritten as

$$\partial s/\partial y^* = B(n_\infty - n_s), \tag{16}$$

with $y^* = y/H$ and $B = \frac{H}{\delta}\frac{D_0}{D}\frac{\rho_0}{\rho_s S_m}$, in which H is the material length in the direction y. The dimensionless number B is reminiscent of the mass transfer Biot number used by Pichler[39]

and Thorell.[40] However, here our number B contains the vapor to bound water density ratio, so that it directly compares a characteristic mass transport by vapor diffusion through the boundary layer (i.e., $\rho_0 D_0/\delta$) to a characteristic mass transport by bound water diffusion in the sample (i.e., $\rho_s S_m D/H$). This allows us to distinguish in a more straightforward way two asymptotic regimes depending on the value of B with respect to 1.

1) "**Equilibrium regime**", for $B << 1$

In that case, $\partial s/\partial y^*$ is negligible, which means that at each step the saturation is homogeneous in the sample (s independent of y), and we have $n_s = n(s)$ at the free surface. As a consequence, the sample mass variation per unit of time writes

$$\rho_s S_m H A \frac{\partial s}{\partial t} = \frac{\mathrm{d}\, M_t}{\mathrm{d}\, t} = -\frac{\rho_0 D_0}{\delta} A(n_\infty - n(s)), \tag{17}$$

in which M_t is the total mass transfer at time t and A is the area of the sample cross-section (in the plane x,z). Thus, remarkably, the (equilibrium) sorption curve may be deduced from the sample mass variation in time:

$$n(s) = n_\infty + \frac{\delta}{\rho_0 A D_0} \frac{\mathrm{d}\, M_t(s)}{\mathrm{d}\, t}. \tag{18}$$

In that case, since the water mass evolution does not depend on D, the apparent sorption or desorption kinetics essentially reflects the sample thickness and the intensity of the air flux, through δ; It does not characterize any intrinsic resistance to water transport or extraction of the material. The equation (18) may be rewritten in the dimensionless form $n(s) = n_\infty + ds/dt^*$ in which $t^* = t/T$ is a reduced time, with $T = \rho_s S_m H \delta/\rho_0 D_0$ the characteristic time of the process. We can remark that this time is simply proportional to the thickness of the boundary layer, i.e., δ, and to the sample thickness. Also note that from equation (18) and since here M_t is proportional to s, it follows that as long as the process occurs for a saturation within the linear

portion of the sorption curve (i.e., typically for $n < 80\%$[65]) the bound water content follows a simple exponential law as a function of time.

2) "**Diffusional regime**", for $B >> 1$

In that case, a significant gradient of concentration develops in the sample, starting from the free surface. As a consequence, we have $n_s \approx n_\infty$. Under these conditions, the sorption or desorption process is no more influenced by the external conditions, it all depends on the ability of the water to be transported throughout the sample, towards or from the free surface. For a constant diffusion coefficient D through the material, the solution for $B \to \infty$ is known analytically and writes:[57]

$$\frac{s - s_0}{s_\infty - s_0} = 1 - \frac{4}{\pi} \sum_{n=0}^{\infty} \frac{(-1)^n}{2n+1} \exp\left\{-(2n+1)^2 \pi^2 Dt/4H^2\right\} \cos \frac{(2n+1)\pi y}{2H}. \qquad (19)$$

in which $s_\infty = s(n_\infty)$ is the bound water concentration at equilibrium with the air flux. The total mass transfer at time t, i.e., M_t, may be expressed as

$$\frac{M_t}{M_\infty} \approx 1 - \sum_{n=0}^{\infty} \frac{8}{(2n+1)^2 \pi^2} \exp\left\{-(2n+1)^2 \pi^2 Dt/4H^2\right\}, \qquad (20)$$

in which M_∞ is the final total water mass transfer at equilibrium, i.e., when the sample has reached a moisture content $S = S(n_\infty)$. Here, the mass transfer only depends on the ratio of the time t and a characteristic time of diffusion in the sample $T^* = H^2/D$. We now have a situation in which the apparent sorption kinetics does not depend on the exact boundary condition, i.e., it does not depend on the value of δ, but instead reflects some intrinsic property of water transport through the thickness of the material, i.e., the inverse of the diffusion coefficient D.

Summary of findings

- The apparent sorption kinetics of a sample subjected to an air flux along its surface depends on the coupling between the air flux and the water diffusion in the material.
- For sufficiently low air flux intensity or small sample thickness, the moisture distribution in the sample remains uniform and evolves towards equilibrium, with a dynamics independent of the intrinsic material properties.
- For sufficiently high air flux intensity or large sample thickness, the moisture distribution is inhomogeneous. The characteristic time of mass transfer is directly related to the diffusion in the material.

Sorption kinetics from controlled air flux test

The above considerations clarify the meaning of sorption kinetics and how it can be related to experimental tests. Basically, the sorption kinetics corresponds to the ability of water to transfer at the surface and diffuse through a material. This may be achieved by placing ourselves in the diffusional regime, for which the diffusive contribution dominates. This diffusion is characterized by the diffusion coefficient. Relevant experiments to determine this coefficient require imposing an air flux that will ultimately reach the sample surface. Under these conditions the controlled boundary conditions are the flow characteristics imposed by some external source at the entrance in an air domain around the sample (see Figure 2). This air flux must be constant, of sufficiently high intensity, and the sample thickness must be sufficiently large for the diffusional regime to be reached. In practice, we also recommend using an air flux perpendicular to the sample surface. The constancy of the air flux ensures a constant pressure on the balance, which will record the sample mass in time (see Figure 3). Moreover, a vertical air flux limits the heterogeneity of the boundary layer thickness along the surface, due to the smaller length of variation (along the sample radius instead

of the sample diameter), and due to the complex air recirculation process. At last, it is worth noticing that although it is directed towards the sample surface the air flux negligibly penetrates the sample. Indeed, the flow may be described thanks to the Darcy's law, which relates the pressure gradient to the mean velocity though a factor inversely proportional to the permeability of the medium. This permeability typically scales with the square of the pore size, and it is even smaller as the tortuosity of the medium is higher.[66,67] As a consequence, the ratio of air flux velocities above (in the container) and inside the sample, resulting from the imposed pressure in the tube, is smaller than the square of the ratio of the pore size in the sample to the tube diameter. The typical values of the tube diameter being in practice around 1 cm while the typical pore size is below 100 μm, the air velocity in the sample is at least four orders of magnitude smaller than the velocity outside the sample. Thus, convection effects inside the sample are negligible.

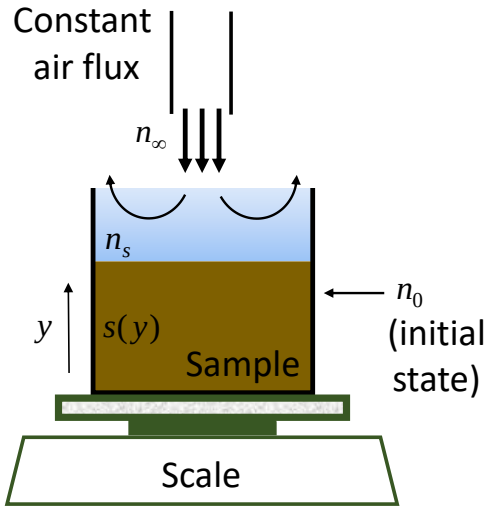

Figure 3: Scheme of the principle of a controlled sorption kinetics test.

Finally, the initially vertical air flux (at the tube exit) essentially induces a tangential flow along the free surface of the sample. The characteristics of this flow obviously vary with the position on this surface. However, according to the above theoretical approach, we know that we can represent the resulting boundary condition in terms of the average vapor flux from the surface with the help of equation (9).

Experimental

Materials and methods

To illustrate the above theoretical predictions, we present data obtained with a typical hygroscopic material, a cellulose fiber stack prepared from cellulose fibers having a strip-like shape with an average length of 300 μm, a width of 10 μm and a thickness of about 1 μm. The sorption curve of this material is shown in.[65] Some fiber amount previously placed during several weeks in a desiccator at a RH of 97%, is then compressed so as to obtain a sample of controlled porosity of 0.72 (void to total volume ratio, noted ε.) Note that under these conditions ε corresponds to the porosity in the saturated state. This compression appears to be sufficient to get a solid material, which will not break during the preparation and the test. After the compression, the material is again placed in a desiccator at 97% RH in order to ensure a homogenously saturated state. Further details on the preparation and characteristics of the material may be found in.[65] The sample is then subjected to a vertical dry air flux ($n_\infty = 0$) according to the scheme shown in Figure 3. The diameter of the cylindrical sample is 5 cm and its thickness is 2.1 cm. The plastic tube from which air arrives has a diameter of 4 mm and its exit is placed at a distance of 4 cm from the sample surface. The air flux is 0.8 L/min. The permeability of this cellulose fiber stack being much smaller than that of the container above its surface, and the paths along the sample axis through the material being dead-ends (due to the container walls), the air flux negligibly penetrates the porosity of the material.

During the test we either follow the mass vs time of the sample or the spatial distribution of bound water with the help of Magnetic Resonance Imaging (MRI), using the Single Point Imaging sequence allowing to measure the local amount of bound water (see article[63]) despite its low NMR relaxation time (typically less than 10 ms).[5] From the latter procedure we get the distribution of bound water, which we call 1D profile, along the sample thickness in the y axis, each data point representing the amount of water in a thin cross-sectional layer.[63,68–70]

Note that in that case the time needed to get a single 1D profile is in the order of one hour. This implies that the sample has to be sufficiently thick for the duration of the process to be much larger than this time.

Boundary layer

Here, as a first step, we test the validity of the expression for the boundary condition (9), i.e., the equation for the mass flux resulting from vapor diffusion through the boundary layer. In that aim, we partially impregnate an initially bound water saturated sample with additional free water, by placing the sample in direct contact with a water bath. In that case, only a very small fraction of water might further penetrate the cellulose in the form of bound water, so that the liquid mostly occupies a fraction of the porosity (i.e., between fibers). The volume fraction of free water in the porosity is noted α, so that the volume fraction of free water in the sample is $\varepsilon\alpha$ (see Figure 4). Under these conditions, the fibers are likely covered with a free water layer of average thickness corresponding to $f(\alpha)R$, in which R is the pore size and f a function increasing from 0 to 1 when α varies from 0 to 1, its detailed variations depending on the pore shapes. Then the characteristic size of the air regions at the pore scale is $(1-\alpha)R$. Thus, we expect some decrease in the roughness of the free surface of the sample as α increases. When $\alpha = 1$, this roughness tends to zero, as the free surface can be considered to be a simple free water layer. Note that in all this approach it is assumed that the characteristic thickness of the boundary layer is much larger than the roughness of the material surface or layer (for a granular sorbent). In that case, the above theoretical developments apply since the RH variations inside the roughness are negligible with respect to the RH variations through the boundary layer. When the roughness is not sufficiently small compared to the theoretical (for a planar surface) boundary layer thickness it becomes necessary to take into account the details of the flow inside the roughness to determine the apparent sorption kinetics.

The results of a drying test under the same conditions of sample size and air flux, and

obtained for different values of α, are presented in Figure 4, in terms of the mass loss as a function of time. We can see that the evolutions for the material partially or fully impregnated with additional free water are quite different from the evolution for the sample only filled with bound water. For the former systems, the mass variations over time are essentially linear, i.e., the slope of the mass vs time curve is constant at least over the first 5 minutes, and does not depend on α (except at longer times, for which the slope for $\alpha = 1$ is slightly larger). We repeated these tests with samples of different porosities (0.7 and 0.8) and found similar results. In contrast, the slope of the curve for the bound water saturated sample (i.e., $\alpha = 0$) continuously decreases.

The behavior of a cellulose sample with a porosity partially filled with free water results from the fact that the free water can be easily transported from depth towards the free surface, driven by capillary effects. As soon as, due to evaporation, some free water is extracted around the free surface, this induces some curvature of the liquid-air interface differing from the average one in depth, which means some unbalance of the Laplace pressure throughout the systems. Following Kelvin's law, the radius r of the free water-air meniscus is related to the RH according to $\ln(n) = -2\sigma V_m/rRT$, with $\sigma = 0.07$ N m^{-1} the water-air surface tension, $V_m = 18$ cm^3 mol^{-1} the molar volume of water, $R = 8.31$ J mol^{-1} K^{-1} the gas constant and $T = 23$ °C the temperature. In our system made of cellulose fibers of typical thickness in the order of a few microns,[65] we expect the minimum size of the menisci to be in the order of one micron, which gives a RH larger than 0.999. In other words, as long as there is a layer of free water covering the fibers, the RH is almost 100%. Then some water flows towards the free surface to reach a new equilibrium situation, i.e., a homogeneous Laplace pressure. If this process is sufficiently fast compared to the drying rate imposed by the air flux,[71] the water concentration remains uniform throughout the system, i.e., equilibrium is continuously maintained, while the average water concentration progressively decreases.[62] This corresponds to the classical situation observed during a first period of drying in various porous media including bead packings,[72,73] clay pastes,[74,75] plaster,[76] nano-porous gels,[77]

biporous systems.[78] Under these conditions, the drying rate remains constant, which is considered to be due to the fact that there remains some significant free water fraction along the free surface, which induces a RH equal to 100% in this region. During this period, some free water is continuously drained towards the surface of the sample thanks to the capillary forces which tend to equilibrate the meniscus size throughout the material.

Actually, our data confirm this analysis, since the drying curves of our samples with different fractions of free water, and the sample filled with free water, exhibit the same drying rate (i.e., slope of mass vs time curve) (see Figure 4). It is remarkable that such a result is obtained despite the roughness variations in these different systems. Thus, these results show that, under these conditions, the roughness plays a minor role on the rate of extraction while the relative humidity induced by the material along the free surface is in any case equal to 100%.

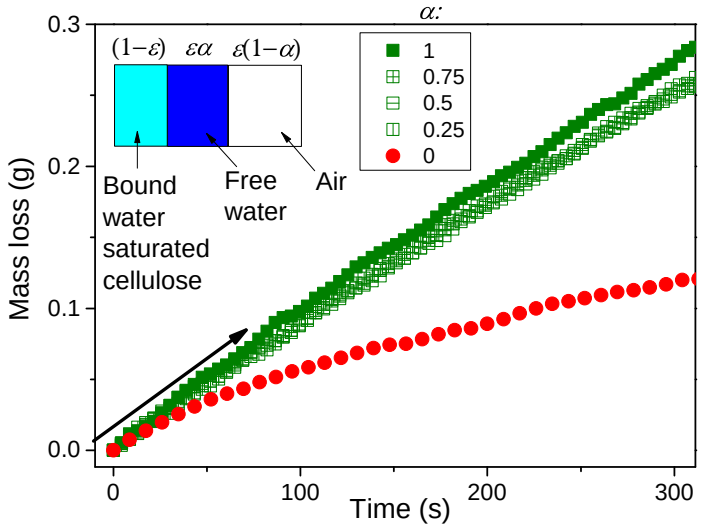

Figure 4: Mass loss vs time for cellulose samples of given porosity ($\varepsilon = 0.8$), with different initial water saturations and subjected to the same dry air flux ($\delta = 1.5$ mm), during the first stages of drying. All samples were saturated with bound water (inside the solid structure) and the porosity was partially filled with free water (see inset picture) with a free water to pore volume fraction equal to α. The straight line with arrow has a slope equal to the common initial slopes of the different mass vs time curves.

In this context, it is particularly interesting to see that the initial rate of extraction, say, over the first few tens of seconds, for the bound water saturated sample is identical to the

rate of extraction for the samples containing free water (see Figure 4). This confirms that the initial rate of extraction is governed by the ambient humidity in the sample, and more precisely by the humidity just around the free surface, but not by some rate of desorption from the fibers or any other property of the material. In the next stage, i.e., after some vapor diffusion from the free surface, some transport of water (vapor and/or bound water) is required from the sample depth, which can be slower than the initial rate of extraction (see Section above).

It is worth noticing that here we could obtain such an agreement between the extraction rate of the samples with different distributions of the water patches in the structure because the sample roughness, or equivalently the water patch size and the characteristic distance between them, which are all in the order of lower than a few tens of microns, are much smaller than the boundary layer thickness (which will appear to be larger than 1 mm for these tests (see below)). Indeed, in that case, the characteristic time for the relative humidity between the patches, i.e., along the sample free surface, to reach 100%, is much smaller than the characteristic time of diffusion through the boundary layer thickness.[79–82]

To conclude, these data confirm the relevance of our approach for the determination of the characteristics of the boundary condition: for a material saturated with bound water one can consider that the RH is equal to 100% along the sample surface as for a sample saturated with free water. Thus, the boundary layer characteristics (i.e., δ) may be determined from the initial rate of extraction when the sample is saturated, so that one can use equation (11) to express the vapor flux at the sample-air interface. Lastly, note that our results show that this approach to the boundary conditions also applies to porous media containing free water.

Sorption kinetics

We then look at the impact of the air flux velocity from experiments under two different boundary conditions: weak dry air flux and very weak air flux at 50% RH. Following the theoretical analysis, we characterize these fluxes of different intensities through the values of

δ they induce, and we determined these values (through equation (9)) from independent mass loss measurements with samples partially filled with free water and under the same conditions otherwise, and using the values $D_0 = 2.7 \times 10^{-5}$ m^2 s^{-1} and $\rho_0 = 0.02$ kg m^{-3}. We found respectively 6.6 and 29 mm for the weak and very weak fluxes. The water distributions over time as determined by MRI for both experiments (see Figure 5) appear to be significantly different for the two tests. For $\delta = 29$ mm and $n_\infty = 0.5$, a slight gradient of concentration rapidly develops from the sample top while in depth, i.e., say, beyond 1 cm from the free surface, the saturation decreases homogeneously (see Figure 5.a). Then the gradient softens and finally we have approximately uniform profiles of decreasing levels over time. In contrast, for $\delta = 6.6$ mm and $n_\infty = 1$, a strong concentration gradient develops immediately from the sample top and progresses inwards while the saturation in depth only weakly decreases (see Figure 5.b). In a next stage, when this gradient has reached the sample bottom, the saturation in depth rapidly decreases.

These results are qualitatively consistent with the expected features in the different situations described above: for a larger δ value, B is smaller so that we expect more flattened profiles, and indeed we can consider that the case $\delta = 29$ mm approaches the equilibrium regime while the case $\delta = 6.6$ mm approaches the diffusional regime. A more detailed analysis requires to fit the diffusion model to these data, which should lead to the determination of the diffusion coefficient. Trying different values for this coefficient we observe that the simple model with a constant value for D (typically around 6×10^{-9} m^2 s^{-1} makes it possible to represent globally well the evolution over time of the average saturation (see Figure 7 Appendix 1), but the predicted shape of the profiles strongly differs from the experimental profiles: the theoretical curvature of the profiles at the approach of the sample top is systematically significantly weaker than the experimental one. Moreover, the water distribution profiles exhibit a feature that is not compatible with a diffusion process considering a single diffusion coefficient value over the whole range of saturation. Such a simple diffusion, i.e., with a constant diffusion coefficient, systematically gives concave profiles at any time during

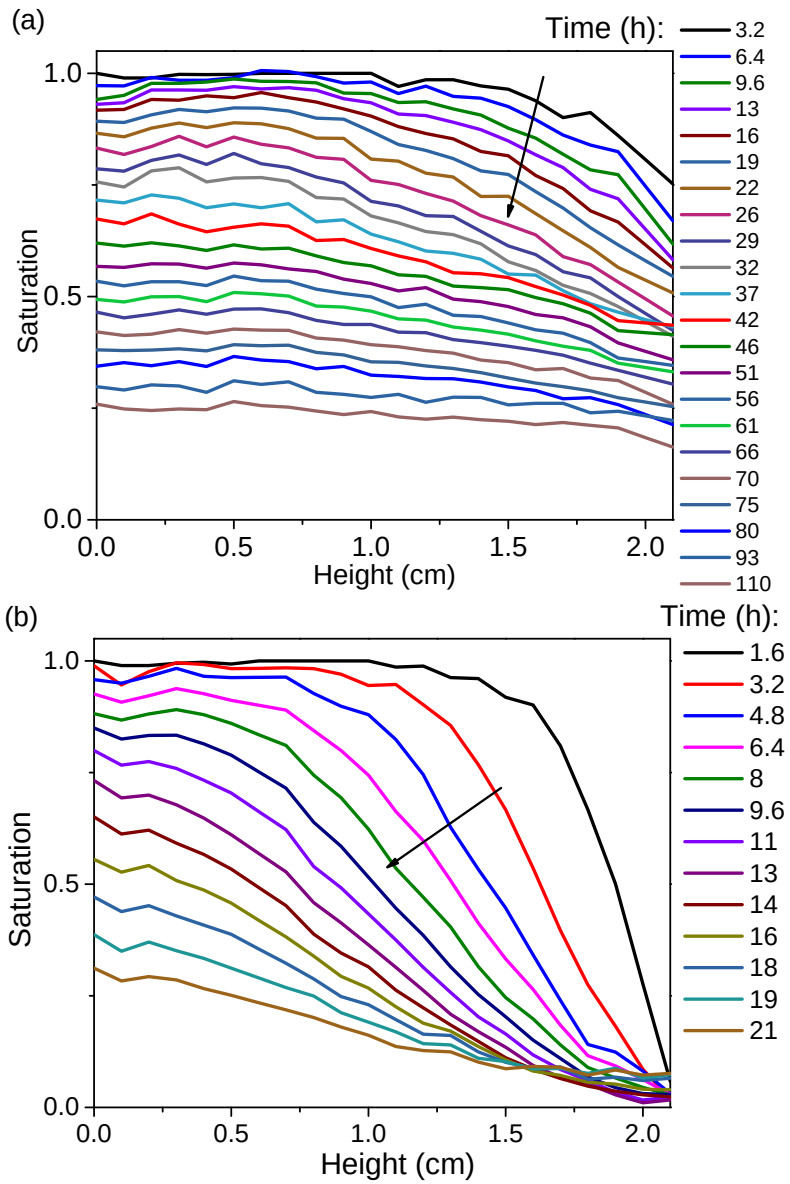

Figure 5: Bound water distribution over time during drying under different conditions: (a) Air flux at 50% RH (δ = 29 mm), (b) Dry air flux (δ = 6.6 mm). The air flux is applied along the top surface situated on the right in the graph. The successive profiles are obtained from MRI measurements at different times during drying. For each profile the measurement duration is 1.6 h.

the process (see Crank[57]), whereas our profiles seem to exhibit an inflection point at the approach of the top surface of the sample (see Figure 5.b). This suggests that there exist at least two domains of different diffusion coefficient values depending on the saturation. More precisely, we expect a larger diffusion coefficient below some saturation around 0.4 which

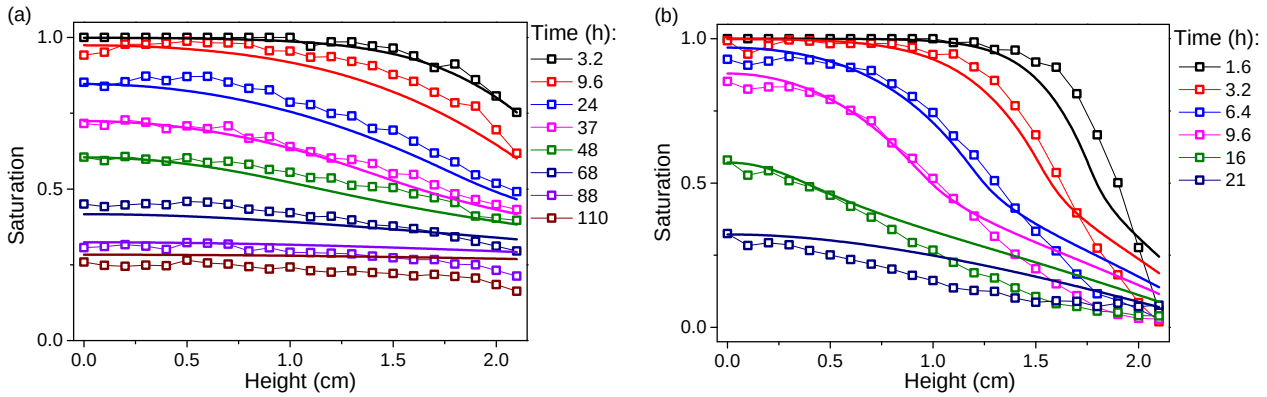

Figure 6: Bound water distribution over time as measured (symbols) at different times (see legend) during drying under (a) air flux at 50% RH and (b) dry air flux (data extracted from Figure 5), and predictions (continuous lines) from of the diffusion model with a two-step diffusion coefficient (see text).

approximately corresponds to the position of the inflection point.

It is out of the scope of this study to discuss in detail the variations of the diffusion coefficient with saturation. Here, we just show the predictions of the diffusion model with a two-step distribution of the diffusion coefficient, i.e., two plateaus linked by a smooth function (see Figure 8 Appendix 2). The solution is obtained by solving numerically the equation (14) with the boundary condition (15), now with a diffusion coefficient D varying with s, along with the condition of no mass flux through the sample bottom and the initial condition $s = s_0$. The plateau levels of the function $D(s)$, chosen after a trial-and-error procedure, i.e., 1.5×10^{-9} m^2 s^{-1} for low saturation and 6×10^{-9} m^2 s^{-1} for high saturation, are able to rather well represent both the correct dynamics of the process and the particular shape of the water distribution over time (see Figure 6). A more complex variation of the diffusion coefficient as a function of the saturation (or even as a function of the gradient of saturation) would likely provide a better agreement but here we show that a two-step model is able to represent the main trends and thus capture the main aspects of the physics of the problem.

Conclusion

We showed from a theoretical analysis that the appreciation of the sorption dynamics from standard measurements in fact essentially relies on a diffusion process inside the sample. Under these conditions, the dynamics of the process may highly depend on the boundary conditions, which can be fully described with the help of a boundary layer thickness which may be determined from the initial flux through the interface or from independent experiments. More precisely, the vapor mass flux going out of the sample is proportional to the difference between the RH of the air flux and along the surface with a factor $(\rho_0 D_0/\delta)$ that only depends on the characteristics of the air flux, namely its density, velocity, viscosity, the diffusion coefficient of vapor through air, and the geometry of the system, including the surface roughness. This vapor mass flux may thus change during the process only if the RH along the surface changes, as a result of the extraction of water from the material. In practice, the factor $\rho_0 D_0/\delta$ may be estimated from independent tests in which the RH along the surface is known, all other things being equal.

Finally, the apparent sorption kinetics results from a competition between (i) the boundary condition, which is controlled by external conditions and (ii) the capacity of bound water to be transported towards the free surface. As a consequence, the various physico-chemical characteristics of the material do not have a direct impact on the sorption kinetics, they should just be taken into account through the possible change they induce on the sorption curve, which characterizes the equilibrium between the RH and the water content, or the diffusion coefficient, which characterizes the transport capacity under a concentration gradient. For sufficiently low air flux intensity or small sample thickness, the moisture distribution in the sample remains uniform and evolves towards equilibrium, with a dynamics independent of the intrinsic material properties. For sufficiently high air flux intensity or large sample thickness, the moisture distribution is inhomogeneous. The characteristic time of mass transfer is directly related to the diffusion in the material. The theory thus shows that the sorption dynamics appreciated from standard tests essentially reflects the air flux

intensity and sample thickness for sufficiently low air flux intensity, and the process of diffusion through the sample for larger air flux intensity. As a consequence, it is more relevant to carry out tests under controlled air flux conditions, i.e., with a fixed air flux at a given RH along the sample surface, in the diffusional regime, and analyze the water mass in the sample as a diffusion taking into account the boundary condition induced by the air flux.

Note that the value of the diffusion coefficient may depend on the saturation. Moreover, its physical origin may be complex, as one can expect both vapor transport through the porous fiber network and bound water diffusion along the fiber network (inside the fibers), as shown from recent experiments with oil-filled fiber stacks.[65] Also, the exchanges between these two phases may play a significant role. The dynamics of these exchanges is in fact the true sorption dynamics which these tests initially aim to explore, but which is hidden by the global diffusion process and, in a second step, i.e., even when the diffusion coefficient has been determined, is just one of the potential processes occurring inside the sample, beside vapor and bound water diffusion. In this context, different diffusion coefficients might be obtained depending on whether the experiment concerns a sorption or a desorption process, which would reflect some hysteresis between the sorption and desorption dynamics, an effect whose origin is still debated for such hygroscopic materials without pre-existing porosity.[83]

Let us finally remark that no assumption is made about the physical characteristics of the material, it can be plain or porous, and it can contain water in any phase or even several phases (e.g., vapor and bound water). Thus, our approach can directly be extended to any such situation. Below we explain the reasons for that.

First of all, our theoretical approach of boundary conditions is still valid in these different cases, since in any event the boundary condition is fixed by the air flux characteristics and the RH along the free surface. We precisely demonstrated this point in the experimental part with a material containing free water, when some desorption tests were carried out with samples partially or fully filled with free water.

Concerning the sorption kinetics, our experiments focus on materials in the "hygroscopic

domain", as the samples have been prepared at a given RH and with such materials we expect that only bound water is present. However, our theoretical analysis, which describes the water transport inside the material with the help of a diffusion equation is general to describe a mass transport due to a gradient of concentration as long as one takes into account that the diffusion coefficient may depend on the local water content (such as equation (14)). The simplest case is the diffusion of vapor through a non-hygroscopic porous material (for which the diffusion coefficient is constant). The case of bound water diffusion inside the solid network (see[65]) is slightly more complex, with a diffusion coefficient possibly depending on saturation. A diffusion equation can still be used when for example vapor and bound water transports occur according to different diffusion processes.[63] At last, the transport of free water resulting from capillary and hydrodynamic effects is also captured by a diffusion equation. Indeed, it is basically described by a Darcy's law which, considering that the gradient of Laplace pressure is proportional to the gradient of saturation (with a factor depending on saturation), is similar to the first Fick's law.

For such transport of free water in drying porous samples the corresponding diffusion coefficient will be larger for smaller pore sizes, so that under given air flux and geometrical conditions we expect to turn from an equilibrium regime to a diffusional regime for a decreasing pore size. The same regime change will occur with a given system when the air flux intensity is increased from a very low to a high value, or by increasing the sample thickness. This is in agreement with the observations of the water distributions over time during the drying of bead packings with pore sizes ranging from 1 mm to a few nanometers[5,72] or clayey materials.[74] Note that an additional complexity with such systems is that, in contrast with hygroscopic systems, at some stage of drying, an apparently dry region of significant thickness can develop below the free surface while there is still water below this region. In this dry region water transport occurs in the form of vapor diffusion so that the whole transport should be described with the help of a two-step diffusion model, i.e., with two different diffusion coefficients respectively for the wet and dry regions.

Appendix 1: Comparison experiment-theory with a simple diffusion model

Here we show a comparison (see Figure 7) of the predictions of a simple diffusion model (i.e., with a constant diffusion coefficient) with our data for the two desorption tests of Figure 5.

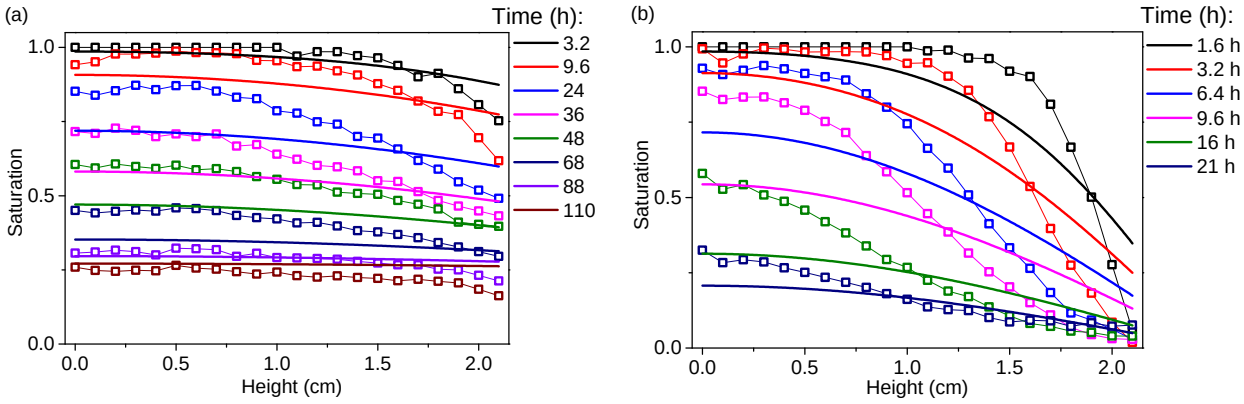

Figure 7: Bound water distribution over time as measured (symbols) at different times (see legend) during drying under (a) air flux at 50% RH and (b) dry air flux (data extracted from Figure 5, and predictions (continuous lines) from of a simple diffusion model with a constant diffusion coefficient 6×10^{-9} m^2 s^{-1}.

Appendix 2: Diffusion coefficient model

Figure 8 shows the variation of the diffusion coefficient as a function of the saturation assumed in the numerical simulations of the diffusion model shown in Figure 6.

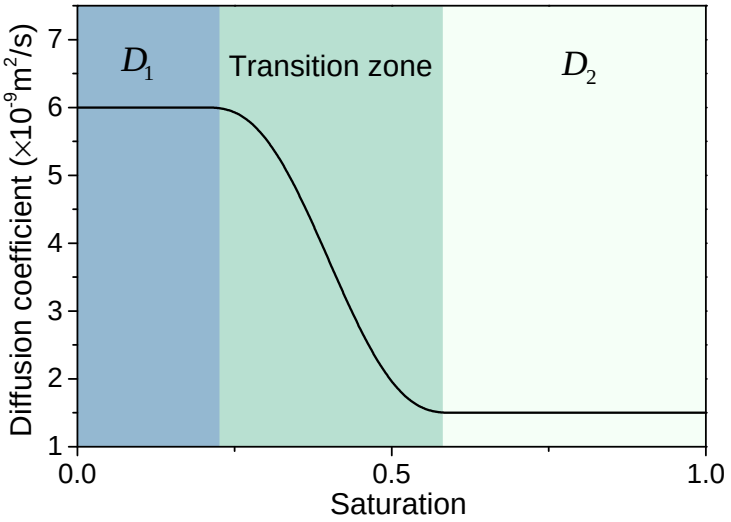

Figure 8: Diffusion coefficient as a function of saturation, as assumed in the theoretical predictions in Figure 6.

Declarations

Ethics approval and consent to participate

Not applicable

Consent for publication

Not applicable

Availability of data and materials

The datasets used and/or analyzed during the current study are available from the corresponding author upon reasonable request.

Competing interests

The authors declare that they have no competing interests

Funding

Funded by the Labex MMCD provided by the national program Investments for the Future of the French National Research Agency (ANR-11-LABX-022), and co-funded by The European Union (ERC PHYSBIOMAT - 101095764). Views and opinions expressed are however those of the authors only and do not necessarily reflect those of the European Union or the European Research Council. Neither the European Union nor the granting authority can be held responsible for them.

Authors' contributions

Y.Z., L.Y., R.S.-B. and B.M. carried out the experiments and analyzed the data. L.B. and P.C. developed the model. Y.Z., L.B. and P.C. wrote the paper. All authors reviewed the manuscript.

References

(1) Berthold, J.; Rinaudo, M.; Salmeń, L. Association of water to polar groups; estimations by an adsorption model for ligno-cellulosic materials. *Colloids and surfaces A: Physicochemical and engineering aspects* **1996**, *112*, 117–129.

(2) O'Neill, H.; Pingali, S. V.; Petridis, L.; He, J.; Mamontov, E.; Hong, L.; Urban, V.; Evans, B.; Langan, P.; Smith, J. C.; others Dynamics of water bound to crystalline cellulose. *Scientific reports* **2017**, *7*, 11840.

(3) Kulasinski, K.; Guyer, R.; Derome, D.; Carmeliet, J. Water adsorption in wood microfibril-hemicellulose system: Role of the crystalline–amorphous interface. *Biomacromolecules* **2015**, *16*, 2972–2978.

(4) Paajanen, A.; Ceccherini, S.; Maloney, T.; Ketoja, J. A. Chirality and bound water in the hierarchical cellulose structure. *Cellulose* **2019**, *26*, 5877–5892.

(5) Maillet, B.; Sidi-Boulenouar, R.; Coussot, P. Dynamic NMR Relaxometry as a Simple Tool for Measuring Liquid Transfers and Characterizing Surface and Structure Evolution in Porous Media. *Langmuir* **2022**, *38*, 15009–15025.

(6) Barnes, J.; Holcombe, B. Moisture sorption and transport in clothing during wear. *Textile Research Journal* **1996**, *66*, 777–786.

(7) Liu, S.-R.; Dai, X.-Q.; Hong, Y. Prediction of the water evaporation rate of wet textile materials in a pre-defined environment. *International Journal of Clothing Science and Technology* **2020**, *32*, 356–365.

(8) Li, Y.; Sun, Y.; Qiu, J.; Liu, T.; Yang, L.; She, H. Moisture absorption characteristics and thermal insulation performance of thermal insulation materials for cold region tunnels. *Construction and Building Materials* **2020**, *237*, 117765.

(9) Yoshino, H.; Mitamura, T.; Hasegawa, K. Moisture buffering and effect of ventilation rate and volume rate of hygrothermal materials in a single room under steady state exterior conditions. *Building and environment* **2009**, *44*, 1418–1425.

(10) Woloszyn, M.; Kalamees, T.; Abadie, M. O.; Steeman, M.; Kalagasidis, A. S. The effect of combining a relative-humidity-sensitive ventilation system with the moisture-buffering capacity of materials on indoor climate and energy efficiency of buildings. *Building and Environment* **2009**, *44*, 515–524.

(11) Le, A. T.; Maalouf, C.; Mai, T. H.; Wurtz, E.; Collet, F. Transient hygrothermal behaviour of a hemp concrete building envelope. *Energy and buildings* **2010**, *42*, 1797–1806.

(12) Dawoud, B.; Aristov, Y. Experimental study on the kinetics of water vapor sorption on selective water sorbents, silica gel and alumina under typical operating conditions of sorption heat pumps. *International Journal of Heat and Mass Transfer* **2003**, *46*, 273–281.

(13) Legrand, U.; Girard-Lauriault, P.-L.; Meunier, J.-L.; Boudreault, R.; Tavares, J. R. Experimental and theoretical assessment of water sorbent kinetics. *Langmuir* **2022**, *38*, 2651–2659.

(14) Roncaroli, F.; Blesa, M. A. Kinetics of adsorption of oxalic acid on different titanium dioxide samples. *Journal of colloid and interface science* **2011**, *356*, 227–233.

(15) Van Heyden, H.; Munz, G.; Schnabel, L.; Schmidt, F.; Mintova, S.; Bein, T. Kinetics of water adsorption in microporous aluminophosphate layers for regenerative heat exchangers. *Applied Thermal Engineering* **2009**, *29*, 1514–1522.

(16) Hossain, M. I.; Glover, T. G. Kinetics of water adsorption in UiO-66 MOF. *Industrial & Engineering Chemistry Research* **2019**, *58*, 10550–10558.

(17) Silva, L. M.; Munoz-Pena, M. J.; Domínguez-Vargas, J. R.; González, T.; Cuerda-Correa, E. M. Kinetic and equilibrium adsorption parameters estimation based on a heterogeneous intraparticle diffusion model. *Surfaces and Interfaces* **2021**, *22*, 100791.

(18) Xu, K.; Ye, H. Theoretical and Experimental Investigation on the Moisture Sorption Kinetics of a PVA/LiCl Composite Membrane in a Dynamic Humidity Environment. *Langmuir* **2020**, *36*, 14453–14460.

(19) Vogt, B. D.; Soles, C. L.; Lee, H.-J.; Lin, E. K.; Wu, W.-l. Moisture absorption and absorption kinetics in polyelectrolyte films: influence of film thickness. *Langmuir* **2004**, *20*, 1453–1458.

(20) Kärger, J.; Vasenkov, S.; Auerbach, S. M. Diffusion in zeolites. *Handbook of Zeolite Science and Technology* **2003**, 341.

(21) Rutherford, S.; Coons, J. Equilibrium and kinetics of water adsorption in carbon molecular sieve: theory and experiment. *Langmuir* **2004**, *20*, 8681–8687.

(22) Montes-H, G.; Géraud, Y. Sorption kinetic of water vapour of MX80 bentonite submitted to different physical–chemical and mechanical conditions. *Colloids and Surfaces A: Physicochemical and Engineering Aspects* **2004**, *235*, 17–23.

(23) Zhao, X.; Wei, X.; Wang, H.; Liu, X.; Zhang, Y.; Zhang, H. Discrepancy of Effective Water Diffusivities Determined from Dynamic Vapor Sorption Measurements with Different Relative Humidity Step Sizes: Observations from Cereal Materials. *Foods* **2023**, *12*, 1470.

(24) Zhang, X.; Zillig, W.; Künzel, H. M.; Mitterer, C.; Zhang, X. Combined effects of sorption hysteresis and its temperature dependency on wood materials and building enclosures–Part I: Measurements for model validation. *Building and Environment* **2016**, *106*, 143–154.

(25) Kinda, J.; Bourdot, A.; Charpin, L.; Michel-Ponnelle, S.; Adia, J.-L.; Thion, R.; Legroux, R.; Benboudjema, F. Experimental and numerical investigation of drying rate impact on moisture loss, exchange coefficient and drying shrinkage of cement paste. *Construction and Building Materials* **2022**, *330*, 127099.

(26) Jamrozowicz, Ł.; Zych, J. Humidity Migration in Surface Layers of Sand Moulds During Processes of Penetration and Drying of Protective Coatings. *Archives of Foundry Engineering* **2022**, *22*, 72–78.

(27) Hill, C. A.; Norton, A.; Newman, G. The water vapor sorption behavior of natural fibers. *Journal of Applied Polymer Science* **2009**, *112*, 1524–1537.

(28) Chen, Q.; Fang, C.; Wang, G.; Ma, X.; Luo, J.; Chen, M.; Dai, C.; Fei, B. Water vapor sorption behavior of bamboo pertaining to its hierarchical structure. *Scientific Reports* **2021**, *11*, 12714.

(29) Glass, S. V.; Boardman, C. R.; Zelinka, S. L. Short hold times in dynamic vapor sorption

measurements mischaracterize the equilibrium moisture content of wood. *Wood Science and Technology* **2017**, *51*, 243–260.

(30) Rode, C.; Peuhkuri, R. H.; Mortensen, L. H.; Hansen, K. K.; Time, B.; Gustavsen, A.; Ojanen, T.; Ahonen, J.; Svennberg, K.; Arfvidsson, J.; others *Moisture buffering of building materials*; Technical University of Denmark, Department of Civil Engineering, 2005.

(31) Nguyen, D. M.; Grillet, A.-C.; Diep, T. M. H.; Thuc, C. N. H.; Woloszyn, M. Hygrothermal properties of bio-insulation building materials based on bamboo fibers and bio-glues. *Construction and Building Materials* **2017**, *155*, 852–866.

(32) Nguyen, D. M.; Grillet, A.-C.; Diep, T. M. H.; Bui, Q.-B.; Woloszyn, M. Characterization of hygrothermal insulating biomaterials modified by inorganic adsorbents. *Heat and Mass Transfer* **2020**, *56*, 2473–2485.

(33) Viel, M.; Collet, F.; Lanos, C. Development and characterization of thermal insulation materials from renewable resources. *Construction and Building Materials* **2019**, *214*, 685–697.

(34) Collet, F.; Chamoin, J.; Pretot, S.; Lanos, C. Comparison of the hygric behaviour of three hemp concretes. *Energy and Buildings* **2013**, *62*, 294–303.

(35) Collet, F.; Pretot, S.; Colson, V.; Gamble, C.; Reuge, N.; Lanos, C. Hygric properties of materials used for ISOBIO wall solution for new buildings. *Academic Journal of Civil Engineering* **2019**, *37*, 349–355.

(36) Mazhoud, B.; Collet, F.; Prétot, S.; Lanos, C. Effect of hemp content and clay stabilization on hygric and thermal properties of hemp-clay composites. *Construction and Building Materials* **2021**, *300*, 123878.

(37) Chennouf, N.; Agoudjil, B.; Alioua, T.; Boudenne, A.; Benzarti, K. Experimental investigation on hygrothermal performance of a bio-based wall made of cement mortar filled with date palm fibers. *Energy and buildings* **2019**, *202*, 109413.

(38) Medjelekh, D.; Ulmet, L.; Gouny, F.; Fouchal, F.; Nait-Ali, B.; Maillard, P.; Dubois, F. Characterization of the coupled hygrothermal behavior of unfired clay masonries: Numerical and experimental aspects. *Building and Environment* **2016**, *110*, 89–103.

(39) Pichler, C.; Lackner, R.; Bader, T.; Perfler, L. Water vapor diffusion properties of Obernkirchener sandstone: Analysis of DVS data. *Construction and Building Materials* **2022**, *347*, 128554.

(40) Thorell, A.; Wadsö, L. Determination of external mass transfer coefficients in dynamic sorption (DVS) measurements. *Drying Technology* **2018**, *36*, 332–340.

(41) Busser, T.; Berger, J.; Piot, A.; Pailha, M.; Woloszyn, M. Comparative study of three models for moisture transfer in hygroscopic materials. *Transport in Porous Media* **2019**, *126*, 379–410.

(42) Reuge, N.; Moissette, S.; Bart, M.; Collet, F.; Lanos, C. Water transport in bio-based porous materials: A model of local kinetics of sorption—application to three hemp concretes. *Transport in Porous Media* **2019**, *128*, 821–836.

(43) Janssen, H.; Blocken, B.; Carmeliet, J. Conservative modelling of the moisture and heat transfer in building components under atmospheric excitation. *International Journal of Heat and Mass Transfer* **2007**, *50*, 1128–1140.

(44) Siau, J. F.; Avramidis, S. The surface emission coefficient of wood. *Wood and Fiber Science* **1996**, 178–185.

(45) Cai, L.; Avramidis, S. A study on the separation of diffusion and surface emission coefficients in wood. *Drying technology* **1997**, *15*, 1457–1473.

(46) Choong, E. T.; Skaar, C. Diffusivity and surface emissivity in wood drying. *Wood and Fiber Science* **1972**, 80–86.

(47) Luikov, A. V. *Advances in heat transfer*; Elsevier, 1964; Vol. 1; pp 123–184.

(48) Erbay, Z.; Icier, F. A review of thin layer drying of foods: theory, modeling, and experimental results. *Critical reviews in food science and nutrition* **2010**, *50*, 441–464.

(49) Thybring, E. E.; Glass, S. V.; Zelinka, S. L. Kinetics of water vapor sorption in wood cell walls: State of the art and research needs. *Forests* **2019**, *10*, 704.

(50) Thybring, E. E.; Boardman, C. R.; Glass, S. V.; Zelinka, S. L. The parallel exponential kinetics model is unfit to characterize moisture sorption kinetics in cellulosic materials. *Cellulose* **2019**, *26*, 723–735.

(51) Murr, A. Water vapour sorption and moisture transport in and across fibre direction of wood. *Cellulose* **2022**, *29*, 4135–4152.

(52) Kohler, R.; Dück, R.; Ausperger, B.; Alex, R. A numeric model for the kinetics of water vapor sorption on cellulosic reinforcement fibers. *Composite Interfaces* **2003**, *10*, 255–276.

(53) Hill, C. A.; Ramsay, J.; Keating, B.; Laine, K.; Rautkari, L.; Hughes, M.; Constant, B. The water vapour sorption properties of thermally modified and densified wood. *Journal of Materials Science* **2012**, *47*, 3191–3197.

(54) Hill, C. A.; Keating, B. A.; Jalaludin, Z.; Mahrdt, E. A rheological description of the water vapour sorption kinetics behaviour of wood invoking a model using a canonical assembly of Kelvin-Voigt elements and a possible link with sorption hysteresis. *Holzforschung* **2012**, *66*, 35–47.

(55) Xie, Y.; Hill, C. A.; Xiao, Z.; Jalaludin, Z.; Militz, H.; Mai, C. Water vapor sorption

kinetics of wood modified with glutaraldehyde. *Journal of applied polymer science* **2010**, *117*, 1674–1682.

(56) Murr, A.; Lackner, R. Analysis on the influence of grain size and grain layer thickness on the sorption kinetics of grained wood at low relative humidity with the use of water vapour sorption experiments. *Wood Science and Technology* **2018**, *52*, 753–776.

(57) Crank, J. *The mathematics of diffusion*; Oxford university press, 1979.

(58) Plazinski, W.; Rudzinski, W. A novel two-resistance model for description of the adsorption kinetics onto porous particles. *Langmuir* **2010**, *26*, 802–808.

(59) Landau, L.; Lifchitz, E. Mécanique des fluides (Physique théorique, tome 6)(traduit du russe). *Mir, Moscou* **1989**,

(60) Bergman, T. L. *Fundamentals of heat and mass transfer*; John Wiley & Sons, 2011.

(61) Bird, R. B.; Stewart, E. S.; Lightfoot, E. N. *Transport Phenomena*; John Wiley & Sons, 2007.

(62) Ben Abdelouahab, N.; Gossard, A.; Ma, X.; Dialla, H.; Maillet, B.; Rodts, S.; Coussot, P. Understanding mechanisms of drying of a cellulose slurry by magnetic resonance imaging. *Cellulose* **2021**, *28*, 5321–5334.

(63) Ma, X.; Maillet, B.; Brochard, L.; Pitois, O.; Sidi-Boulenouar, R.; Coussot, P. Vapor-sorption coupled diffusion in cellulose fiber pile revealed by magnetic resonance imaging. *Physical Review Applied* **2022**, *17*, 024048.

(64) Zhou, M.; Caré, S.; Courtier-Murias, D.; Faure, P.; Rodts, S.; Coussot, P. Magnetic resonance imaging evidences of the impact of water sorption on hardwood capillary imbibition dynamics. *Wood Science and Technology* **2018**, *52*, 929–955.

(65) Zou, Y.; Maillet, B.; Brochard, L.; Coussot, P. Fast transport diffusion of bound water in cellulose fiber network. *Cellulose* **2023**, 1–16.

(66) Scheidegger, A. E. *The physics of flow through porous media*; University of Toronto press, 1957.

(67) Daïan, J.-F. *Equilibrium and transfer in porous media 1: Equilibrium states*; John Wiley & Sons, 2014.

(68) Cocusse, M.; Rosales, M.; Maillet, B.; Sidi-Boulenouar, R.; Julien, E.; Caré, S.; Coussot, P. Two-step diffusion in cellular hygroscopic (vascular plant-like) materials. *Science Advances* **2022**, *8*, eabm7830.

(69) Penvern, H.; Zhou, M.; Maillet, B.; Courtier-Murias, D.; Scheel, M.; Perrin, J.; Weitkamp, T.; Bardet, S.; Caré, S.; Coussot, P. How bound water regulates wood drying. *Physical Review Applied* **2020**, *14*, 054051.

(70) Zhou, M.; Caré, S.; King, A.; Courtier-Murias, D.; Rodts, S.; Gerber, G.; Aimedieu, P.; Bonnet, M.; Bornert, M.; Coussot, P. Wetting enhanced by water adsorption in hygroscopic plantlike materials. *Physical Review Research* **2019**, *1*, 033190.

(71) Coussot, P. Scaling approach of the convective drying of a porous medium. *The European physical journal B-condensed matter and complex systems* **2000**, *15*, 557–566.

(72) Thiery, J.; Rodts, S.; Weitz, D.; Coussot, P. Drying regimes in homogeneous porous media from macro-to nanoscale. *Physical Review Fluids* **2017**, *2*, 074201.

(73) Maillet, B.; Dittrich, G.; Huber, P.; Coussot, P. Diffusionlike drying of a nanoporous solid as revealed by magnetic resonance imaging. *Physical Review Applied* **2022**, *18*, 054027.

(74) Faure, P.; Coussot, P. Drying of a model soil. *Physical Review E* **2010**, *82*, 036303.

(75) Ben Abdelouahab, N.; Gossard, A.; Rodts, S.; Coasne, B.; Coussot, P. Convective drying of a porous medium with a paste cover. *The European Physical Journal E* **2019**, *42*, 1–12.

(76) Seck, M. D.; Van Landeghem, M.; Faure, P.; Rodts, S.; Combes, R.; Cavalié, P.; Keita, E.; Coussot, P. The mechanisms of plaster drying. *Journal of Materials Science* **2015**, *50*, 2491–2501.

(77) Thiery, J.; Rodts, S.; Keita, E.; Chateau, X.; Faure, P.; Courtier-Murias, D.; Kodger, T.; Coussot, P. Water transfer and crack regimes in nanocolloidal gels. *Physical Review E* **2015**, *91*, 042407.

(78) Lerouge, T.; Maillet, B.; Coutier-Murias, D.; Grande, D.; Le Droumaguet, B.; Pitois, O.; Coussot, P. Drying of a compressible biporous material. *Physical Review Applied* **2020**, *13*, 044061.

(79) Suzuki, M.; Maeda, S. On the mechanism of drying of granular beds mass transfer from discontinuous source. *Journal of chemical engineering of Japan* **1968**, *1*, 26–31.

(80) Lehmann, P.; Or, D. Effect of wetness patchiness on evaporation dynamics from drying porous surfaces. *Water Resources Research* **2013**, *49*, 8250–8262.

(81) Shahraeeni, E.; Lehmann, P.; Or, D. Coupling of evaporative fluxes from drying porous surfaces with air boundary layer: Characteristics of evaporation from discrete pores. *Water Resources Research* **2012**, *48*.

(82) Haghighi, E.; Shahraeeni, E.; Lehmann, P.; Or, D. Evaporation rates across a convective air boundary layer are dominated by diffusion. *Water Resources Research* **2013**, *49*, 1602–1610.

(83) Chen, M.; Coasne, B.; Guyer, R.; Derome, D.; Carmeliet, J. Role of hydrogen bonding in hysteresis observed in sorption-induced swelling of soft nanoporous polymers. *Nature Communications* **2018**, *9*, 3507.

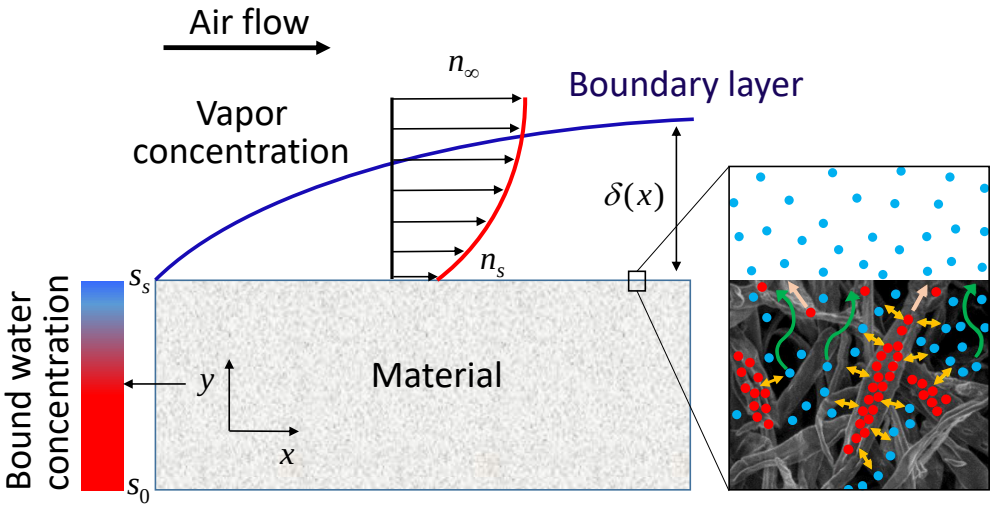
Air flow
n_∞
Boundary layer
Vapor concentration
$\delta(x)$
n_s
s_s
Bound water concentration
Material
y
x
s_0

TOC Graphic